Nanogranular metallic Fe–oxygen deficient $TiO_{2-\delta}$ composite films: a room temperature, highly carrier polarized magnetic semiconductor

2008 J. Phys.: Condens. Matter 20 195206

(http://iopscience.iop.org/0953-8984/20/19/195206)

J. Phys.: Condens. Matter **20** (2008) 195206 (6pp) doi:10.1088/0953-8984/20/19/195206

Nanogranular metallic Fe–oxygen deficient $TiO_{2-\delta}$ composite films: a room temperature, highly carrier polarized magnetic semiconductor

S D Yoon[1], A Widom[2], K E Miller[3], M E McHenry[3], C Vittoria[1] and V G Harris[1]

[1] Center for Microwave Magnetic Materials and Integrated Circuits, Department of Electrical and Computer Engineering, Northeastern University, Boston, MA 02115, USA
[2] Department of Physics, Northeastern University, Boston, MA 02115, USA
[3] Department of Material Science and Engineering, Carnegie Mellon University, Pittsburgh, PA 15213, USA

Received 9 January 2008, in final form 12 March 2008
Published 11 April 2008
Online at stacks.iop.org/JPhysCM/20/195206

Abstract

Nanogranular metallic iron (Fe) and titanium dioxide ($TiO_{2-\delta}$) were sequentially deposited on (100) lanthanum aluminate ($LaAlO_3$) substrates in a low oxygen chamber pressure using a pulsed laser ablation deposition (PLD) technique. By sequential deposition, ≈10 nm diameter metallic Fe spherical grains were suspended within a $TiO_{2-\delta}$ matrix. The films show ferromagnetic behavior with a saturation magnetization of 3100 G at room temperature. Our estimate of the saturation magnetization based on the size and distribution of the Fe spheres agreed with the measured value. The film composite structure was characterized as a p-type magnetic semiconductor at 300 K with a carrier density of the order of $\approx 10^{22}$ cm^{-3}. The hole carriers were excited at the interface between the nanogranular Fe and $TiO_{2-\delta}$ matrix, similar to holes excited in the metal/n-type semiconductor interface commonly observed in metal-oxide-semiconductor (MOS) devices. From the large anomalous Hall effect measured in these films, we observed that the holes at the interface were strongly spin polarized. Structure and magnetotransport properties suggested that these PLD films have potential spintronics applications.

(Some figures in this article are in colour only in the electronic version)

1. Introduction

The search for semiconductors exhibiting magnetism at room temperature has been long and unyielding. However, recently much progress has been made towards this goal [1–7]. By doping a host semiconductor material with transition metal substitutions, dilute ferromagnetic semiconductors have been produced with Curie temperatures (T_c) as high as 160 K [1]. Hall effect measurements below T_c showed evidence for carriers being spin polarized, raising hopes for spintronics applications. Specifically, metallic manganese was doped into gallium arsenide whereby the carriers were strongly spin polarized [1].

We have previously reported the magnetic and transport properties of magnetic semiconductor films of $TiO_{2-\delta}$, where δ indicates the degree of oxygen deficiency or defects in the film [8–10]. The Curie temperature, $T_c \sim 880$ K, was well above room temperature with a saturation magnetization, $4\pi M_S$, of ≈400 G. Titanium dioxide, TiO_2, is a well known wide band gap oxide semiconductor, belonging to the group IV–VI semiconductors, described in terms of an ionic model of Ti^{4+} and O^{2-} [11–15]. Its intriguing dielectric properties allow its use as a gate insulator material in field-effect transistors (FETs) [16]. Also, TiO_2 is characterized to be an n-type semiconductor with an energy gap varying in the range $3\text{ V} < \frac{\Delta}{e} < 9\text{ V}$ depending on sample preparation [11–15]. Films of

$TiO_{2-\delta}$ on substrates of (100) lanthanum aluminate ($LaAlO_3$) were deposited by a pulsed laser ablation deposition (PLD) technique at various oxygen chamber pressures ranging from 0.3 to 400 mTorr. The origin of the presence of Ti^{2+} and Ti^{3+} (as well as Ti^{4+}) ions was postulated as a result of the low oxygen chamber pressure during the film's growth [9]. Oxygen defects gave rise to valence states of Ti^{2+} and Ti^{3+} (in the background of Ti^{4+}) whereby double exchange between these sites dominated. The same carriers involved in double exchange also gave rise to impurity donor levels accounting for the transport properties of the film. The dilute number of carriers were polarized in an external applied magnetic field, yet the magnetic moment was still rather small [10]. For example, normal Hall resistivity was measured to be much larger than the anomalous Hall resistivity [10]. In order to increase the anomalous contribution to the Hall effect and thereby increase the number of polarized carriers, we have fabricated films consisting of nanogranular (NG) metallic iron (Fe) in a semiconducting $TiO_{2-\delta}$ matrix. The intent was to introduce a substantial magnetization component internally to the semiconductor $TiO_{2-\delta}$.

The basic difference between our film composite and the previously reported magnetic semiconductors used by others is that in our films the NG Fe exist in a metallic state, whereas in the magnetic semiconductors prepared by others the transition metals exist as metal oxides and often oxide clusters [4–7]. This major difference is important in terms of the magnetic and transport properties of the magnetic semiconductor produced by us and others [4–7]. For example, NG metallic Fe contains a significantly higher moment and Curie temperature than any other transition metal oxides. Also, the presence of NG metallic Fe allows for the creation of a reservoir of electrons in the conduction band and, therefore, holes in the $TiO_{2-\delta}$ matrix. As electrons from the conduction band of $TiO_{2-\delta}$ are thermally introduced into the Fe conduction band, holes are created in $TiO_{2-\delta}$ much like in the junctions of NG metal/semiconductor interfaces or in metal-oxide-semiconductor (MOS) devices [17]. Conduction of holes occurs in the $TiO_{2-\delta}$ host. This mechanism gives rise to lower resistivity at high temperatures in contrast to the pure $TiO_{2-\delta}$ reported earlier [9, 10] where the carriers were only electrons. No such mechanism is possible in magnetic semiconductors doped with transition metal oxides. We report the following magnetic properties for our composite films: room temperature saturation magnetization, $4\pi M_S \approx 3100$ G; T_c above 800 K; and nearly 100% of the carriers were spin polarized. Experimental results, discussions, and concluding remarks follow.

2. Experimental results and analysis

Thin films consisting of nanogranular metallic Fe and $TiO_{2-\delta}$ were deposited by a pulsed laser ablation deposition technique from binary targets of TiO_2 and metallic Fe on (100) $LaAlO_3$ substrates. Targets of TiO_2 and Fe were mounted on a target rotator driven by a servomotor and synchronized with the trigger of the pulsed excimer laser, $\lambda = 248$ nm. In each deposition cycle, the ratio of laser pulses incident upon the TiO_2 target to those upon the Fe target was 6:1. This technique has been described previously as alternating target laser ablation deposition (AT-LAD). The substrate temperature, laser energy density, and pulse repetition rate were maintained at 700 °C, ~8.9 J cm^{-2}, and 1 Hz, respectively. The deposition was carried out in a partial pressure of oxygen of $\sim 10^{-5}$ Torr in order to induce defects in the TiO_2 host. There were a total of 4200 laser pulses (3600 pulses on the TiO_2 target and 600 pulses on the Fe target) for each film, resulting in a thickness of approximately 200 nm as measured by a Dek-Tek step profilometer.

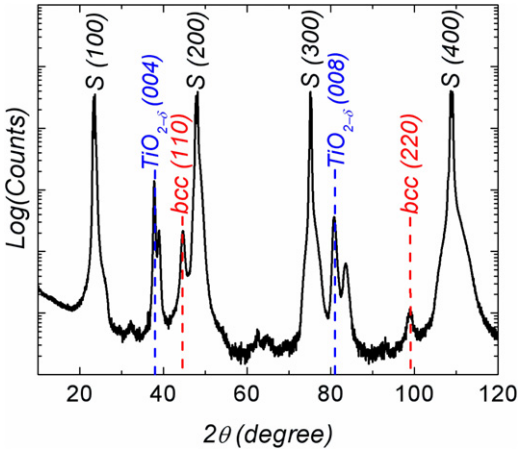

Figure 1. A typical x-ray diffraction pattern showing the presence of (001) anatase $TiO_{2-\delta}$ and (110) metallic bcc FE phases.

Crystallographic and micrographic properties of the AT-LAD films were measured using x-ray diffractometry (XRD) and transmission electron microscopy (TEM). Results indicate phases of anatase TiO_2 and metallic body-centered-cubic (bcc) Fe. The (001) plane of anatase $TiO_{2-\delta}$ and the (110) plane of bcc Fe phases are clearly exhibited in the XRD pattern [18, 19] shown in figure 1. The peak appearing near $2\theta = 32.20°$ could not be readily indexed but may originate from the presence of iron oxide (FeO or Fe_2O_3) or ilmenite ($FeTiO_3$) phases.

In figure 2, reflection electron diffraction (upper inset) supports the existence of the epitaxial $TiO_{2-\delta}$ film host, while the TEM image (lower inset) reveal the presence of NG metallic Fe particles suspended within the $TiO_{2-\delta}$ host. A JOEL 2000EX high resolution transmission electron microscope (HRTEM) was used in the analysis. An HRTEM image, shown in figure 2, illustrates NG metallic Fe spheres formed at the interface between the $TiO_{2-\delta}$ film and the $LaAlO_3$ substrate. The average diameter of the NG spheres was measured to be ≈10–15 nm as shown in the TEM image. The image suggests that the AT-LAD process may lead to the segregation of metallic Fe spheres in the host $TiO_{2-\delta}$. The average atomic ratio of Fe to Ti ions in the AT-LAD films was obtained using energy dispersive x-ray spectroscopy (EDXS) within a Hitachi S-4800 scanning electron microscope. Findings indicate ≈6 ± 0.5% of Fe ions are present in the 1 × 1 cm^2 area of the films.

For steady currents and with the magnetic field **H** directed normal to the film plane, the resistance tensor, **R**, whose

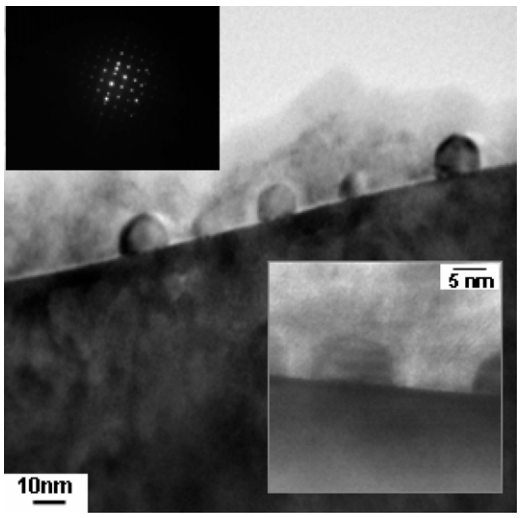

Figure 2. TEM images of a representative film consisting of nanogranular metallic Fe in the $TiO_{2-\delta}$ host.

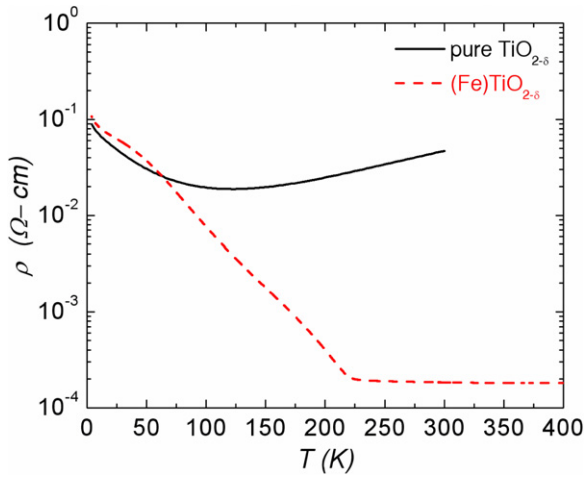

Figure 3. Resistivity, ρ as a function of temperature, T, for the nanogranular Fe in $TiO_{2-\delta}$ film (dashed line) and the pure $TiO_{2-\delta}$ (solid line) from [10].

elements measured in the plane of the film may be written as [20]

$$\mathbf{R} = \begin{bmatrix} R_{xx} & R_{xy} \\ -R_{yx} & R_{yy} \end{bmatrix} = \frac{1}{t}\begin{bmatrix} \rho & \rho_{\mathrm{H}} \\ -\rho_{\mathrm{H}} & \rho \end{bmatrix}, \qquad (1)$$

wherein ρ and ρ_{H} represent, respectively, the normal and Hall resistivities. The ρ as a function of temperature for the film was measured in an applied field of $\mathbf{H} = 0$ Oe, see figure 3. We note that the value of $\rho(T)$ was quite small at high temperatures. The $\rho(T)$ behavior for the pure $TiO_{2-\delta}$ film [9] (solid line) is also shown in figure 3, exhibiting a typical metal–insulator crossover in the temperature range of 4–300 K. In contrast to the ρ for pure $TiO_{2-\delta}$, ρ for the composite of NG metallic Fe and $TiO_{2-\delta}$ film is a factor of 1000 lower and is nearly constant for temperatures between 225 and 400 K. The temperature variations are of the characteristic form expected from metal semiconductor interfaces. The ρ value at 300 K was measured to be 183 $\mu\Omega$ cm and is about a factor of 20 larger than the resistivity of metallic Fe [21].

The presence of these unique transport properties in the NG metallic Fe spheres embedded in $TiO_{2-\delta}$ films has been modeled as coexisting electronic structures of both semiconducting $TiO_{2-\delta}$ and metallic Fe. We have modeled the mechanism for transport in this composite film in a sketch shown in figure 4 [17, 22, 23]. A common chemical potential, i.e. Fermi energy, in both $TiO_{2-\delta}$ and metallic Fe implies that the conduction band of $TiO_{2-\delta}$ overlaps with the metallic Fe conduction band. Since the Fermi energy in metallic Fe is about 4.3 eV above the bottom of the conduction energy band, it implies that the energy band gap (3 eV) of $TiO_{2-\delta}$ overlaps the Fe conduction band. The electrons hopping between Ti^{2+} and Ti^{3+} sites would find a conduit into the metallic conduction band, leaving behind holes near the top of the $TiO_{2-\delta}$ conduction band. A small potential barrier must exist at the interface. This is illustrated schematically in figure 4(a). As noted in figure 2, the NG metallic Fe spheroids are isolated or disconnected, implying that conduction in the $TiO_{2-\delta}$ is via hole conduction. This can be also explained by the presence of a contact potential at the interface between the NG Fe spheres and anatase $TiO_{2-\delta}$, as described in [20]. In order to remove the electron trough from the surface of metallic Fe, work must be done thermodynamically. According to [20], Poisson's equation for the potential $\Phi(x)$ along the x-axis normal to the interface between NG Fe and the $TiO_{2-\delta}$ implies

$$\begin{aligned} -\Phi''(x) &= 4\pi\rho(x), \\ \varpi &= \int_{-\infty}^{\infty} x\rho(x)\,\mathrm{d}x = -\frac{1}{4\pi}\int_{-\infty}^{\infty} x\Phi''(x)\,\mathrm{d}x, \\ \Phi(\infty) - \Phi(-\infty) &= V_{\mathrm{c}} = 4\pi\varpi, \end{aligned} \qquad (2)$$

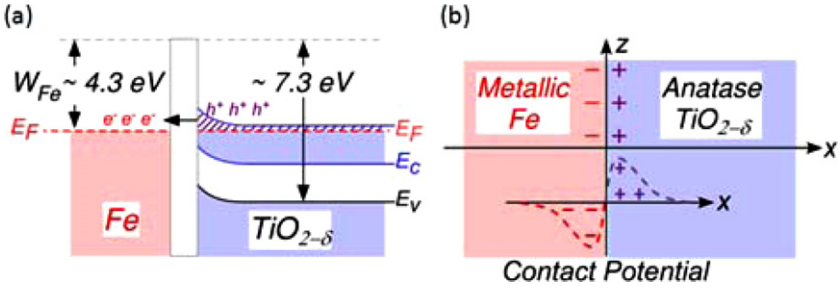

Figure 4. (a) Local energy band structure of nanogranular metallic Fe and semiconducting $TiO_{2-\delta}$. (b) Schematic shows the contact potential between metallic Fe and $TiO_{2-\delta}$.

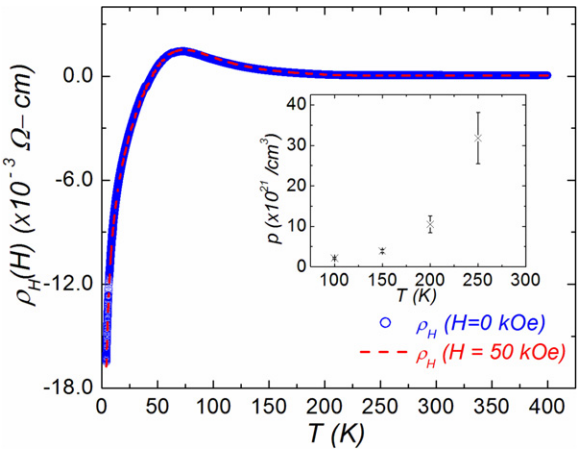

Figure 5. Hall resistivity, ρ_{H}, versus temperature for $H = 0$ (circle symbol) and $H = 50$ kOe (dashed line) for nanogranular metallic Fe in the $TiO_{2-\delta}$ film. Inset shows the carrier density as a function of temperature.

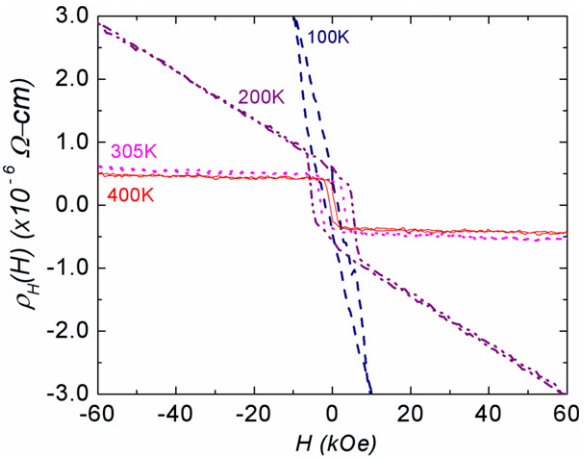

Figure 6. Hall resistivity, $\rho_{\mathrm{H}}(H)$, versus H at different temperatures.

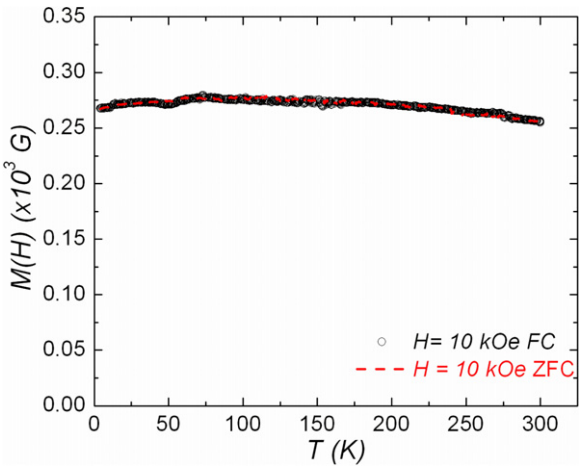

Figure 7. Static magnetization, $M(H, T)$, versus temperature for $H = 10$ kOe aligned normal to the film plane.

wherein ϖ is defined to be a dipole moment unit contact area and V_{c} is the contact potential. The schematic of the contact potential at the interface is shown in figure 4(b).

Electron conduction between metallic spheres may not be possible (see figure 2). The Hall resistivity is plotted as a function of temperature in figure 5. As the temperature is lowered the density of holes rapidly decreases until at low temperatures holes no longer dominate the transport process. At high temperatures, the number of holes relative to electron carriers in pure $TiO_{2-\delta}$ has increased by a factor of 1000 and the mass of holes is approximately 10 times larger than the electron mass [10]. Also in figure 5, the carrier hole density, p, is plotted as a function of temperature. In order to calculate p, we simply use the following relation

$$\rho_{\mathrm{H}} = R_0 B + 4\pi M R_{\mathrm{S}} \qquad \text{and} \qquad R_0 = \frac{1}{pec}, \tag{3}$$

wherein R_0 and R_{S} are the normal and anomalous Hall coefficients, respectively. In figure 6, $\rho_{\mathrm{H}}(H)$ is shown to scale linearly with magnetic field for temperatures below 300 K. The slope of ρ_{H} versus H gives rise to the normal Hall coefficient which corresponds to the first term in equation (3), where the hole carrier density, p, may be deduced. The polarity of the carriers was also confirmed to be that of holes, as we performed Seebeck effect measurements on the same composite films. For temperatures well above 250 K, p is governed by the second term in equation (3), the anomalous Hall coefficient. Equation (3) may re-written as [24]

$$\rho_{\mathrm{H}} = \frac{H}{pec} + \left(\frac{1}{pec} + R_{\mathrm{S}}\right) 4\pi M \qquad \text{and} \qquad R_{\mathrm{S}} \gg R_0. \tag{4}$$

The anomalous Hall effect is dominant at high temperatures ($T \geqslant 250$ K) and the second term in equation (4) is constant for $4\pi M = 4\pi M_{\mathrm{S}}$, the saturation magnetization.

The spontaneous magnetization, $M(H, T)$, was measured to be nearly constant as a function of temperature, as shown in figure 7. The measurement was performed with an external dc magnetic field of 10 kOe applied normal to the film plane (i.e. out-of-plane measurement). The film can be fully saturated with a field of ≈6.6 kOe, since the coercive field was measured to be 2.0 kOe. Field-cooled (FC) and zero-field-cooled (ZFC) $M(H, T)$ data presented in figure 7 showed no difference, which implied that no spin glass effects were present in the films. There are two sources for magnetism in this composite structure: (1) ferromagnetism in $TiO_{2-\delta}$ and (2) ferromagnetism in metallic Fe spheres. The ferromagnetism in $TiO_{2-\delta}$ is due to double exchange as calculated in [25], and it gives rise to a relatively small saturation magnetization at room temperature (∼400 G). Based on the data presented in figure 2, we estimate a sphere density of 0.125 to 0.25 $\times$ 10^{18} spheres cm^{-3} and a sphere diameter between 10 and 15 nm. This implies that the loading factor of metallic Fe in the composite film is of the order of 0.05–0.25 which corresponds to 1100–5100 G for the saturation magnetization of the composite. This compares

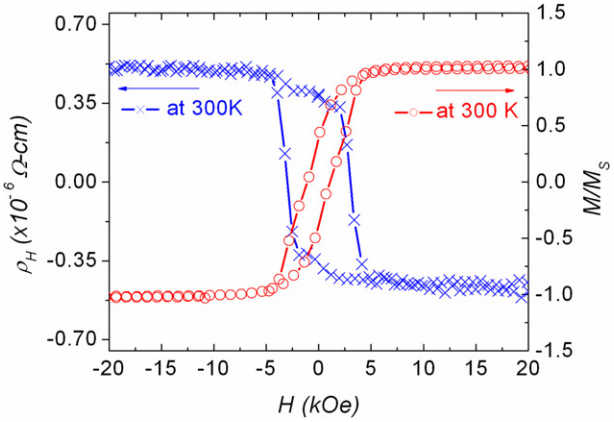

Figure 8. A typical anomalous Hall hysteresis loop, $\rho_{\rm H}(H)$ (symbol (X)), with a magnetic hysteresis loop (symbol (O)) at 300 K.

with a measured value of 3100 G. The magnetic moment can be presumably increased by the addition of more iron. We have measured the transverse magnetoresistivity, $\rho(H)$, and Hall resistivity, $\rho_{\rm H}(H)$, as a function of magnetic field between -90 and $+90$ kOe. The normal resistivity exhibits negative magnetoresistivity defined as, $\Delta f = \frac{\rho(H)-\rho(0)}{\rho(0)}$, where $\Delta f \approx -1\%$ for temperatures of 100 and 200 K. Δf is negligible for temperatures above 300 K. However, plots of $\rho_{\rm H}(H)$, shown in figure 6, clearly demonstrate that saturation effects at temperatures near room temperature are a result of the hole carrier density increasing toward saturation levels (see figure 5). Notice that plots of $\rho_{\rm H}(H)$ at $T \geqslant 200$ K exhibit clear hysteresis behavior similar to ferromagnetic hysteresis loops. Interestingly, saturation for both $\rho_{\rm H}(H)$ and $\frac{M}{M_{\rm S}}$ normalized magnetization occurred at exactly the same external magnetic field value of ≈6.6 kOe, see figure 8, which is approximately equal to $\frac{4\pi M_{\rm S}}{3}$, the demagnetizing field of Fe spheres at room temperature. These data also show a smaller coercive field for the $\frac{M}{M_{\rm S}}$ hysteresis loop than for the $\rho_{\rm H}(H)$ hysteresis loop. The difference in hysteresis loops is due to the fact that the Fe spheroids give rise to dipole internal magnetic fields. In order to reverse the magnetization in each sphere, an external field is required to overcome this internal field. Hence, the coercive field is approximately constant with temperature as it scales with magnetization. In the Hall resistivity measurement the coercive field is strongly temperature dependent, since there are two contributions to the resistivity measurement: (1) the normal Hall resistivity contribution, which is not hysteretic with respect to **H**, and (2) the anomalous Hall effect (AHE) which is hysteretic with **H**, since this effect is proportional to the magnetization. At high temperatures the AHE contribution dominates the resistivity measurement in contrast to low temperatures where the normal Hall contribution dominates. Thus, spin polarization, as reflected in $\rho_{\rm H}(H)$ (see figure 8), correlates extremely well with the magnetic hysteresis loop, implying that the magnetized Fe spheroids are polarizing the carriers.

3. Conclusions

The plots of $\rho_{\rm H}(H)$ at $T < 200$ K exhibit unsaturated hysteretic behavior, see figure 6. This transition between unsaturated and fully saturated $\rho_{\rm H}(H)$ hysteresis behavior was also reported and correlated with hole carrier density related to Ruderman–Kittel–Kasuya–Yoshida (RKKY) theory by previous researchers [1, 26]. Their estimation of threshold hole density for carrier spin polarization transition was $p = 3 \times 10^{20}$ cm^{-3}, which indicated a transition from unsaturated ($p < 3 \times 10^{20}$ cm^{-3}) to saturated ($p \geqslant 3 \times 10^{20}$ cm^{-3}) hysteresis behavior [1, 24, 26]. Our estimation of hole carrier density of the films was $p \approx 2.1 \times 10^{21}$ and ≈10×10^{21} cm^{-3} at $T = 100$ and 200 K, respectively. The film exhibited strong polarization and hysteresis behavior as a function of applied field at 300 K. Since anomalous Hall effects may be observed in the presence of spontaneous magnetization [27, 28], we infer that about ≈10^{22} cm^{-3} hole carriers are polarized by an applied field **H**. This indicates that nearly all of the carriers were polarized by the spontaneous magnetization at $T = 300$ K. According to figure 8, the carrier polarization correlated very well with the magnetic hysteresis loop of the Fe spheroids. Usually, the magnetization and Hall resistivity (as measured via anomalous Hall measurements) saturate for the same magnetic field direction [1]. This is contrary to figure 8. Figure 8 indicates that the carrier polarization is not affected by external fields up to 3.0 kOe, which can be an advantage for memory device applications [29, 30]. However, if the shape of the particles embedded within the host could be formed as needles, it would imply that the spin polarization of carriers would occur in an external magnetic field below ∼0.1 kOe.

In summary, magnetic and magnetotransport data for films of nanogranular metallic Fe and oxygen defect $TiO_{2-\delta}$ are reported. The essence of this paper showed that conduction carriers of the films were strongly coupled to residual magnetic moments of metallic Fe grains in the nanocomposite structure. The dramatic reduction of normal resistivity ($\rho(T)$) of the films is a consequence of two factors: (1) oxygen defects in the $TiO_{2-\delta}$ host induced electron hopping; (2) electrons from the $TiO_{2-\delta}$ were introduced into the conduction band of Fe to create holes in $TiO_{2-\delta}$, similar to a metal oxide semiconductor (MOS) structure. As a result, the number of carriers increased at room temperature. The holes in $TiO_{2-\delta}$ were polarized due to the presence of ferromagnetic nanogranular metallic Fe, where the carrier polarized density was measured to be $\geqslant 3.0 \times 10^{22}$ cm^{-3}. Therefore, spintronics and spin dependent memory elements for computational applications may be based upon the results presented here.

Acknowledgments

This research was supported by the National Science Foundation (DMR 0400676) and the Office of Naval Research (N00014-07-1-0701).

References

[1] Ohno H 1998 *Science* **281** 951
[2] Ueda K, Tahata H and Kawai T 2001 *Appl. Phys. Lett.* **79** 988

[3] Masumoto Y *et al* 2001 *Science* **291** 854
[4] Pearton S J *et al* 2003 *Mater. Sci. Eng.* R **40** 137
[5] Chambers S A and Farrow R F C 2003 *MRS Bull.* **28** 729
[6] Zutic I, Fabian J and Sarma D 2004 *Rev. Mod. Phys.* **76** 32
[7] Coey J M D, Venkatesan M and Fitzgerald C B 2005 *Nat. Mater.* **4** 173
[8] Hong N H *et al* 2006 *Phys. Rev.* B **73** 132404
[9] Yoon S D *et al* 2006 *J. Phys.: Condens. Matter* **18** L355
[10] Yoon S D *et al* 2007 *J. Phys.: Condens. Matter* **19** 326202
[11] Earle M 1942 *Phys. Rev.* **61** 56
[12] Breckenridge R G and Hosler W R 1953 *Phys. Rev.* **91** 793
[13] Daude N, Gout C and Jouanin C 1977 *Phys. Rev.* B **15** 3229
[14] Pascual J, Camassel J and Mathieu H 1978 *Phys. Rev.* B **18** 5606
[15] Tang H *et al* 1993 *Solid State Commun.* **87** 847
[16] Campbell S A *et al* 1999 *IBM J. Res. Dev.* **43** 383
[17] Streetman B G 1990 *Solid State Electronic Devices* (Englewood Cliffs, NJ: Prentice-Hall) chapter 8, p 301
[18] Swanson H E, Doukhan J C and Ugrinic G M 1955 *Natl Bur. Stand. (U.S.), Circ.* **5** 539
[19] Howard C J, Sabine T M and Dickson F 1991 *Acta Crystallogr.* B **47** 462
[20] Landau L D and Lifshitz E M 1982 *Electrodynamics of Continuous Media* (Oxford: Elservier–Butterworth-Heinemann) chapter 4, p 1984
[21] Weast R C and Astle M J 1982 *CRC Handbook of Chemistry and Physics* 63rd edn (Boca Raton, FL: CRC) p E-81
[22] Knotek M L and Feibelman P J 1978 *Phys. Rev. Lett.* **40** 964
[23] Zhang Z, Jeng S P and Henrich V 1991 *Phys. Rev.* B **43** 12004
[24] Hurd C M 1972 *The Hall Effect in Metals and Alloys* (New York: Plenum) chapter 5
[25] Zuo X, Yoon S, Yang A, Vittoria C and Harris V G 2008 *J. Appl. Phys.* **103** 07B911
[26] Story T *et al* 1986 *Phys. Rev. Lett.* **56** 777
[27] Chien C L and Westgate C R 1980 *The Hall Effect and its Applications* (New York: Plenum)
[28] Karplus R and Luttinger J M 1954 *Phys. Rev.* **95** 1154
[29] Prinz G 1998 *Science* **282** 1660
[30] Wolf S A *et al* 2001 *Science* **294** 1488